

Isolation, Structure Elucidation, and Biological Activity of Virgineone from *Lachnum virgineum* Using the Genome-Wide *Candida albicans* Fitness Test

John Ondeyka,[†] Guy Harris,[†] Deborah Zink,[†] Angela Basilio,[‡] Francisca Vicente,[‡] Gerald Bills,[‡] Gonzalo Platas,[‡] Javier Collado,[‡] Antonio González,[‡] Mercedes de la Cruz,[‡] Jesus Martin,[‡] Jennifer Nielsen Kahn,[†] Stefan Galuska,[†] Robert Giacobbe,[†] George Abruzzo,[†] Emily Hickey,[†] Paul Liberator,[†] Bo Jiang,[§] Deming Xu,[§] Terry Roemer,^{§,†} and Sheo B. Singh^{*,§}

Natural Products Chemistry, Merck Research Laboratories, Rahway, New Jersey 07065, Centro de Investigación Básica, Merck Sharp & Dohme de España, S. A., Madrid, Spain, Infectious Diseases, Merck Research Laboratories, Rahway, New Jersey 07065, and Center of Fungal Genetics, Merck Frosst Canada Ltd., Montrel, Quebec, Canada

Received August 16, 2008

A glycosylated tetramic acid, virgineone (**1**), was isolated from saprotrophic *Lachnum virgineum*. The antifungal activity of the fermentation extract of *L. virgineum* was characterized in the *Candida albicans* fitness test as distinguishable from other natural products tested. Bioassay-guided fractionation yielded **1**, a tyrosine-derived tetramic acid with a C-22 oxygenated chain and a β -mannose. It displayed broad-spectrum antifungal activity against *Candida* spp. and *Aspergillus fumigatus* with a MIC of 4 and 16 $\mu\text{g/mL}$, respectively. Virgineone was also identified in a number of *Lachnum* strains collected from diverse geographies and habitats.

Infections caused by pathogenic fungi (e.g., *Candida albicans* and *Aspergillus fumigatus*) are life-threatening, particularly to immunocompromised populations.¹ There are three main therapeutic options for such infections: azoles (e.g., fluconazole),² macrocyclic polyenes (e.g., amphotericin),³ and candins (e.g., caspofungin, micafungin, and anidulafungin).⁴ Each treatment option has limitations to its utility, thus creating a need for new antifungal agents.

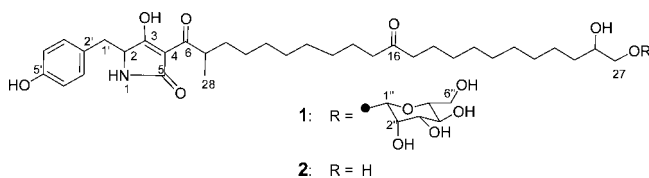
Natural products have provided many of the antifungal leads and drugs and continue to be the most prolific source for novel and chemically diverse leads. Rediscovery of known compounds, however, poses a significant challenge in natural product research and calls for ingenious dereplication strategies enabling efficient discovery of new bioactive compounds. Critical to this is the fusion of new sources of natural products and bioactivity detection in crude extracts. In a two-prong approach, we expanded our efforts to isolate microorganisms from diverse geographical regions and habitats in combination with improved high-throughput fermentation methods.⁵ In parallel, we adapted a chemogenetic assay in *C. albicans*, the fitness test, that profiles the biological activities (targets and/or mechanisms of action, in many cases) of antifungal compounds and extracts.^{6–8} Combining these two resources, we discovered, from fungi, a new class of novel antifungal compounds, parnafungins, that inhibit mRNA polyadenylation with a broad spectrum of antifungal activity with *in vivo* efficacy in a murine model of candidiasis.^{9,10}

The *C. albicans* fitness test (CaFT) exploits the diploid nature of the pathogen. For the majority of genes, deletion of one allele is phenotypically neutral. However, antiproliferative compounds, at sublethal concentrations, may induce variations in growth that are restricted to only a subset of the heterozygotes. As demonstrated, target- or mechanism-specific inhibitors elicit phenotypic variations (i.e., hypersensitivity and resistance) in heterozygotes that are indicative of mechanisms of action (MOAs).⁸ Conversely, the collective responses (i.e., “signature” profiles) of heterozygotes may reflect different aspects of MOAs of synthetic compounds¹¹ and bioactive compounds present in the crude extracts from natural

sources.^{9,10} In the reported version of the CaFT, a pool of ~2900 heterozygous deletion strains was used in the assay. In each of the heterozygotes, specific barcodes are introduced in the deleted allele that enable strain identification by DNA microarrays and phenotypic assay *en masse*.

CaFT profiling can be used in a number of ways to aid natural product research. By matching CaFT profiles of crude extracts to those in a compendium of characterized compounds, it is possible to remove extracts containing known actives prior to chemical fractionation. On the other hand, if a profile suggests a novel target and/or mechanism of action, the corresponding extract could be prioritized for chemical dereplication and fractionation, as in the case of parnafungin, in which the original extract produced a CaFT profile similar to that of cordycepin, but containing additional information indicative of mechanistic novelty.⁹ Occasionally, antifungal actives yield CaFT profiles that do not sufficiently reflect the targets or the precise MOAs. Some of them nevertheless contain enough biological information to indicate that the bioactivities are distinguishable from known compounds and other extracts. If LCMS analyses fail to identify known actives in these extracts, they could then be fractionated. The CaFT provides a means to verify the purified bioactivities.

Applying the CaFT to crude extracts from microbial sources, we identified a number of natural product extracts that were predicted to possess novel bioactivities. Here we report the isolation, structural elucidation, and biological activity of a new antifungal compound, virgineone (**1**), produced by the fungus *Lachnum virgineum*.



Results and Discussion

Identification of a Novel Bioactivity Produced by *Lachnum virgineum* and Related *Lachnum* Strains. Screening of microbial natural product extracts against wild-type *C. albicans* identified a large number of extracts that showed growth inhibition of *C. albicans*. While testing these broths in the CaFT, we identified

* Corresponding author. Fax: 1(732) 594-6880. E-mail: sheo_singh@merck.com.

[†] NPC, Rahway.

[‡] CIBE, Spain.

[†] Infectious Diseases, Rahway.

[§] Center of Fungal Genetics, Merck Frosst, Canada.

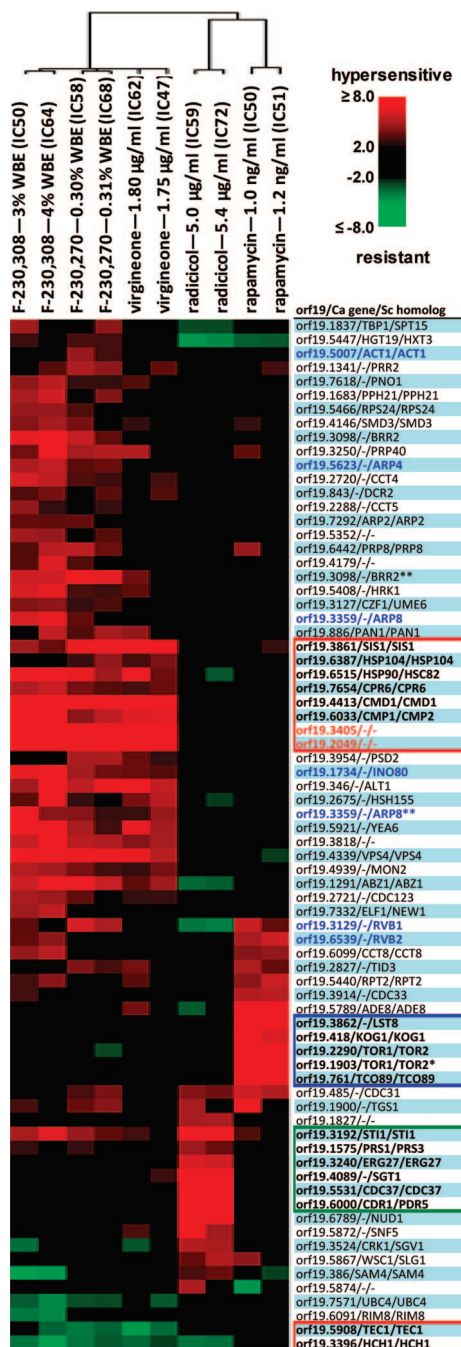


Figure 1. CaFT profiles of crude fungal extracts (F-230,270 and F-230,308), virgineone (**1**), radicicol, and rapamycin. Two independent CaFT experiments with comparable inhibitory concentrations (ICs) were selected for each active. The normalized z-scores (statistic appraisal of the responsiveness,⁸ hypersensitivity with z-score > 0, and resistance < 0) were compiled and analyzed by Cluster 3.0. The strains were selected with the absolute value of z-scores no less than 3.5 in at least two experiments. They (74 in total) were grouped by hierarchical clustering using the centroid linkage method and displayed in TreeView with the scale of the heat map (z-scores) indicated in the top right corner. The hierarchical linkage of each experiment is shown on the top. The highlighted strains include those that are specific to these extracts and virgineone (red boxes; see text for detailed description), radicicol (green box, described in ref 8, with the exception of *STII*, encoding a cochaperone of HSP90), and rapamycin (blue box, the TOC complex, * indicating an independent heterozygote in which the 5' portion of the ORF was deleted). Also highlighted, in blue (bold), are components of the INO80-chromatin remodeling complex. Other independently constructed strains are indicated by two asterisks (**).

several extracts that yielded highly related CaFT profiles that were distinct from the larger screening set and consisted largely of heterozygous deletion strains for genes involved in multiple cellular processes (Figure 1). Of particular interest, it is likely that the two extracts, F-230,270 and F-230,308, elicited the calmodulin-dependent stress response, as suggested by induced hypersensitivity of heterozygotes for calmodulin (*CMD1*), calcineurin (the regulatory subunit of the phosphatase, *CMP1*), heat-shock protein 90 (*HSP90*), and its associated cochaperones (*SIS1*, *HSP104*, and *CPR6*). Although the components of this stress response pathway are targeted by known compounds derived from microbial sources, including FK506 (produced by *Streptomyces tsukubaensis*), cyclosporine A (*Tolypocladium inflatum*), and radicicol (*Pochonia chlamydosporia*), all of them and rapamycin (*S. hygroscopicus*, targeting the TOR pathway) generated largely nonoverlapping CaFT profiles (Figure 1 and data not shown). Furthermore, the collective hypersensitivity of strains for the aforementioned genes, together with two *C. albicans* specific genes (*orf19.2049* and *orf19.3405*), and the resistance of *HCH1* (for another HSP90 cochaperone) heterozygote are restricted to these three and other related extracts (see below). They showed no responses to other compounds or natural products tested in the CaFT (data not shown). These data suggested that the biological activities and the compounds within these extracts were likely unique within the screening set examined. The extract of fungus F-230,270 was selected for bioassay-guided isolation of the active principle.

The producer fungal strain F-230,270 was isolated from an unidentified plant in the province of Santa Cruz, Argentina. It was further identified as *Lachnum virgineum* by ITS and 28S rDNA analysis (Supporting Information, Figures S1 and S2). The antifungal activity of its metabolites was first detected in a fermentation extract grown in a microfermentation array employing eight media,⁵ only one of which yielded significant antifungal activity against wild-type *C. albicans* (data not shown). Further screening encountered at least nine other highly related *Lachnum* strains that produced the same active component (Supporting Information, Table S1).

Isolation and Structure Elucidation of Virgineone (1). A fermentation of F-230,270 was scaled up to 1 L and extracted with acetone. A portion of the acetone extract, equivalent to 50 mL of broth, was subjected to a standardized, prioritization scale fractionation on Mitsubishi CHP20Y. A single antifungal activity eluting in fractions 10–15 (of 28 in total) was obtained. Extracts from the related culture F-230,308 exhibited similar behavior when subjected to prioritization scale fractionation with activity eluting in fractions 13–15. Interestingly, small-scale elution-extrusion countercurrent fractionation (EECC)¹⁰ of the rich cuts from both extracts resulted in stationary phase disruption and hence no separation. Scale-up isolation was accomplished by capture on Amberchrom followed by successive chromatographies of the antifungal active fractions on Sephadex LH20 and reversed-phase C₈ HPLC to afford 326 mg (326 mg/L) of virgineone (**1**) as a colorless powder.

The UV spectrum of **1** showed absorption maxima at λ_{\max} 201, 229, 242 (sh), and 281 nm. HRESIFTMS produced a formula of C₄₀H₆₃NO₁₂. The ¹³C NMR spectrum displayed many overlapping signals particularly in the aliphatic region of the spectrum but supported the overall formula. The IR spectrum exhibited absorption bands for hydroxy groups, an aliphatic chain, and a ketone. The ¹³C NMR spectrum in DMSO-*d*₆ displayed 28 (12 overlapping) resonances, which were eventually assigned to 20 methylenes, 12 methines, and one methyl by a DEPT spectrum. The remaining seven were quaternary carbons (Table 1). The ¹H NMR spectrum supported these assignments, and careful integration indicated the presence of 63 protons. The ¹H NMR spectrum showed the presence of four aromatic protons as two pairs of doublets at δ_{H} 6.56 (2H, d, *J* = 8.0 Hz) and 6.92 (2H, d, *J* = 8.0 Hz), which displayed DFQ-COSY cross-peaks to each other (Table 1). The methine at

Table 1. ¹H (500 MHz) and ¹³C (125 MHz) NMR Assignments of Virgineone (**1**) and Aglycone (**2**)

position	1 δ _C DMSO- <i>d</i> ₆		1 δ _H (mult, <i>J</i> in Hz) DMSO- <i>d</i> ₆	HMBC (H→C) DMSO- <i>d</i> ₆	1 δ _H (mult, <i>J</i> in Hz) CD ₃ OD	2 δ _C DMSO- <i>d</i> ₆	2 δ _H (mult, <i>J</i> in Hz) DMSO- <i>d</i> ₆
1		NH	7.33 (s)	C-2, 3, 4			
2	60.8	CH	3.57 (brt, 5.5)	C-3, 5, 2'	3.74 (dd, 7.5, 4.5)	62.1	4.04 (m)
3	193.6	C°				191.7	
4	99.6	C°				100.4	
5	177.1	C°				175.5	
6	197.5	C°				194.5	
7	38.4	CH	3.65 (m)	C-6, 8, 9, 28	3.67 (m)	35.8	3.42 (m)
8	33.0	CH ₂	1.05 (m) 1.50 (m)		0.95 (m) 1.45 (m)	33.0	1.4–1.5 (m)
9	27.0	CH ₂	1.20 (m)		1.24–1.29 (m)	26.6	1.2 (m)
10–13	29.0	CH ₂	1.20 (m)	C-14, 15, 10–13	1.24–1.29 (m)	28.5–29.2	1.2 (m)
14	23.3	CH ₂	1.40 (m)	C-16, 12–13, 15	1.52 (m)	23.2	1.42 (m)
15	41.8	CH ₂	2.34 (apparent q, 7.0)	C-13, 14, 16	2.43 (m)	41.8	2.36 (m)
16	210.0	C°				210.5	
17	41.8	CH ₂	2.34 (apparent q, 7.0)	C-16, 18, 19	2.43 (m)	41.8	2.36 (m)
18	23.3	CH ₂	1.40 (m)	C-16, 17, 19	1.52 (m)	23.2	1.42 (m)
19–24	29.0	CH ₂	1.20 (m)		1.24–1.29 (m)	28.5–29.2	1.2 (m)
25	33.4	CH ₂	1.20 (m) 1.35 (m)	C-26, 23–24, 27	1.18 (m) 1.65 (m)	33.4	1.4–1.5 (m)
26	69.0	CH	3.53 (m)		3.73 (m)	71.0	3.36 (m)
27	73.4	CH ₂	3.28 (dd, 10.0, 7.0) 3.62 (dd, 10.0, 4.0)	C-25, 26, 1'' C-25, 1''	3.43 (dd, 10, 6.0) 3.86 (dd, 10, 2.5)	66.0	3.20 (2H,m)
28	17.6	CH ₃	0.82, (d, 7.0)	C-6, 7, 8		17.0	0.95 (d, 7.0)
1'	36.8	CH ₂	2.59 (dd, 13.5, 6.0) 2.78 (dd, 13.5, 3.5)	C-2, 3, 2', 3' C-2, 3, 2', 3'	2.98 (brd, 14.5) 2.74 (br)	35.8	2.82 (brd, 5.0)
2'	127.6	C°				125.6	
3'/7'	130.4	CH	6.92 (d, 8.0)	C-1', 7'/3', 4'/6', 5'	7.00 (d, 8.5)	130.6	6.97 (t, 8.5)
4'/6'	114.6	CH	6.56 (d, 8.0)	C-2', 5', 6'/4'	6.62 (d, 8.5)	114.7	6.65 (t, 8.5)
5'	155.5	C°				155.9	
1''	100.6	CH	4.36 (brs)	C-27, 2'', 5''	4.55 (d, 1.0)		
2''	70.4	CH	3.64 (br)	C-1'', 3'', 4''	3.88 (dd, 3.0, 1.0)		
3''	73.6	CH	3.23 (br)	C-1'', 3'', 5''	3.45 (dd, 9.5, 3.0)		
4''	67.1	CH	3.26 (m)	C-1'', 3'', 5''	3.55 (t, 9.5)		
5''	77.5	CH	3.0 (ddd, 9.0, 6.0, 2.0)	C-1'', 3'', 4'', 6''	3.20 (ddd, 9.5, 6.0, 2.5)		
6''	61.4	CH ₂	3.42 (m) 3.66 (m)		3.70 (dd, 12.0, 6.0) 3.87 (dd, 12.5, 3.0)		
4'-OH		OH	9.95 (br)	C-4'/6', 5'			9.15 (brs)
2''-OH		OH	4.22 (br)				
3''-OH		OH	4.5 (br)	C-2'', 3''			
4''-OH		OH	4.67 (d, 5.0)	C-3'', 4'', 5''			
6''-OH		OH	4.41 (br)				

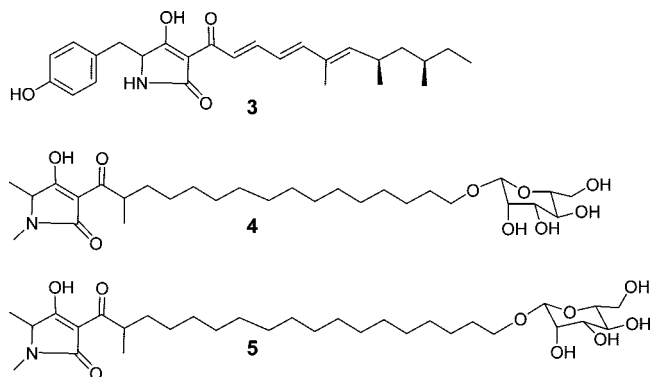
δ_{H} 3.57 (1H, brt, $J = 5.5$ Hz) exhibited DQF-COSY correlations to the benzylic methylene protons resonating at δ_{H} 2.78 (1H, dd, $J = 13.5, 3.5$ Hz) and δ_{H} 2.59 (1H, dd, $J = 13.5, 6.0$ Hz). The benzylic methylene protons displayed HMBC correlations to the methine carbon C-2 (δ_{C} 60.8), C-3 (δ_{C} 193.6), and the aromatic carbons C-2' (δ_{C} 127.6) and C-3' (δ_{C} 130.4); the phenolic OH group resonated at δ_{H} 9.95, which showed HMBC correlation to C-4'/6' and C-5', thus establishing the presence of a *para*-hydroxy benzyl group connected to a methine.

The ¹³C NMR spectrum showed three keto carbons (δ_{C} 193.6, 177.1, and 197.5) and a upfield shifted quaternary carbon (δ_{C} 99.6), which are generally present in tetramic acid moieties.¹² The methine (C-2) resonance at δ_{C} 60.8 and a nitrogen in the formula of **1** corroborated the presence of a tetramic acid moiety, which was confirmed by HMBC correlations of NH (δ_{H} 7.33) to C-2, C-3 (δ_{C} 193.6) and C-4 (δ_{C} 99.6). The methine proton H-2 exhibited HMBC correlations to C-3, C-5 (δ_{C} 177.1) and C-2', confirming the presence of a *para*-hydroxy benzyl tetramic acid moiety. The downfield shifted methine proton H-7 (δ_{H} 3.65, m) showed DQF-COSY correlations to the methyl group (δ_{H} 0.82, d, $J = 7$ Hz) and a pair of methylene proton multiplets (δ_{H} 1.05 and 1.50). These methylene protons displayed DQF-COSY correlations to the methylene protons that resonated as a part of the methylene envelope. The methyl group H₃-28 showed HMBC correlations to C-6 (δ_{C} 197.5), C-7 (δ_{C} 38.4), and C-8 (δ_{C} 33.0), and H-7 displayed HMBC correlations to C-6, C-8, C-9, and C-28, thus establishing the connectivity of the tetramic acid moiety with the aliphatic chain.

Analysis of the remaining resonances suggested the presence of an aliphatic ketone (δ_{C} 210.0), an anomeric methine (δ_{H} 4.36 and

δ_{C} 100.6), five oxymethines, and two oxymethylenes. DQF-COSY correlations of these protons suggested the presence of a hexose moiety and confirmed the presence of the remaining oxymethine and oxymethylene at the terminal end of the aliphatic chain. The 2'' proton of the hexose moiety showed small couplings with H-1'' ($J = 1$ Hz) and H-3'' ($J = 3$ Hz), consistent with the presence of an axial hydroxy group at C-2'' and, therefore, suggesting that the hexose moiety was β -mannose. This conclusion was corroborated by coupling constants measured in CD₃OD (Table 1) and is consistent with values reported for mannosyl tetramic acids.^{13,14} Like many tetramic acids, the NMR spectrum of **1** exhibited signal broadenings¹² for a large number of resonances and required both solvents (DMSO-*d*₆ and CD₃OD) for critical assignments. The anomeric proton (δ_{H} 4.36) displayed HMBC correlations with C-2'' and C-5'' and C-27, confirming the glycosidation at C-27.

HRESIFTMS analysis showed a major fragment ion at m/z 588.3881 due to loss of the mannose moiety. The exact location of the ketone group in the chain could not be assigned by NMR methods due to degeneracy of the ¹H and ¹³C NMR chemical shifts, but was assigned at C-16 by HRESIFTMS-MS fragmentation of the aglycone **2**, which was prepared by acid hydrolysis of **1**. The HRESIFTMS analysis of **2** displayed a protonated parent ion at m/z 588.3886 and key fragment ions at m/z 372.2172 and 400.2121 due to cleavages of the C–C bonds before (C15/C16) and after (C16/C17) the keto group (Figure 2). The origin of these fragment ions was confirmed by MS-MS analysis. On the basis of the spectroscopic data, the acyl tetramic acid structure **1** was assigned for virgineone.



Virgineone (**1**) is likely derived from condensation of tyrosine and a C-24 β -keto acid. The left-hand portion of **1** has been reported as a structural part of several natural products exemplified by militarinone C (**3**).¹⁵ The dihydroxy C-22 long acyl alkyl chain with or without a ketone group has not been reported. Epicoccamides A (**4**) and D (**5**), C-18 and C-20 β -keto acid and alanine derived tetramic acids, have been reported.^{13,14} Militarinone C was isolated from the fungus *Cordyceps militaris* and has been shown to have very weak neurotoxic activity in PC-12 cells.¹⁵ Epicoccamide A (**4**) was isolated from jellyfish-derived strains of *Epicoccum purpurascens*, and epicoccamide D (**5**) was isolated from an *Epicoccum* sp. associated with the wood-decay fungus *Pholiota squarrosa*.^{13,14} These compounds demonstrated cytotoxic activities against the HeLa cell line.

Antifungal Activity of Virgineone (1). The CaFT profile of purified virgineone (Figure 1) was consistent with that originally observed with crude acetone extracts. Thus the *in vitro* *C. albicans* growth inhibition assay was an appropriate surrogate bioassay for isolation of the active component. Virgineone exhibited broad-spectrum antifungal activity against a number of key pathogenic fungal strains (Table 2). There was little variation in potency among the *Candida* spp. examined, with MIC values of 4–16 $\mu\text{g}/\text{mL}$. Virgineone was equally potent against two filamentous fungi, *Aspergillus fumigatus* and *Trichophyton mentagrophytes*. The *in vitro* antifungal activity of **1** was reduced at least 4-fold in the presence of mouse or human serum. It was tested for efficacy in an *in vivo* disseminated *C. albicans* MY1055 mouse (DBA/2) model at 100 and 50 mg/kg dosed twice daily intraperitoneally (ip). It showed 100% mortality at 100 mg/kg and 40% mortality at 50 mg/kg dose levels. No reduction in fungal cfu was observed in surviving mice compared to the control, suggesting lack of efficacy. Similar dosing of uninfected mice did not show any mortality perhaps due to immune modulation. Caspofungin was used as a control. The aglycone (**2**) did not show any antifungal activity at 32 $\mu\text{g}/\text{mL}$.

CaFT profiling mechanistically differentiates virgineone from other natural products (radicalol, cyclosporine A, FK506, and rapamycin) that target the calmodulin–calcineurin–HSP90 pathway¹⁶ (Figure 1 and data not shown). This was supported by the lack of potentiation of fluconazole by **1**, which was achieved in the combination of fluconazole with cyclosporine A (data not shown). However, it is not possible to predict the precise target or MOA of **1** based solely on the CaFT profiles. Nonetheless, they contain additional genes that are of interest. Noticeably, one of the *C. albicans* specific genes, *orf19.2049*, encodes for potential membrane protein, while the other, *orf19.3405*, has been recently described as a zinc-finger transcription factor (Zcf18p) related to

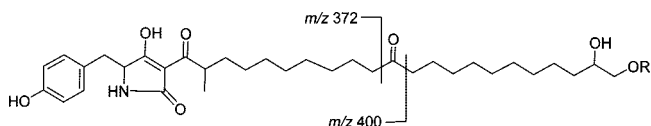


Figure 2. Mass fragmentation of **1** and **2**.

Table 2. Antifungal Activity (MIC, $\mu\text{g}/\text{mL}$) of Virgineone (**1**) and Caspofungin

test organism	strain no.	virgineone	caspofungin
<i>C. albicans</i>	MY1055	8	0.5
<i>C. albicans</i> + 50% mouse serum	MY1055	>32	0.25
<i>C. glabrata</i>	MY1381	8	0.25
<i>C. parapsilosis</i>	ATCC22019	8	0.5
<i>C. lusitanae</i>	MY1396	4	<0.03
<i>C. krusei</i>	ATCC6258	16	1
<i>A. fumigatus</i>	MF5668	8	32
<i>A. fumigatus</i> + 50% human serum	MF5668	>32	32
<i>T. mentagrophytes</i>	MF7004	8	32
<i>S. aureus</i>	MB2865	16	>32

S. cerevisiae Lys14p (CGD, www.candidagenome.org) but not essential for viability.¹⁷ Another group of genes are for components of the INO80 chromatin remodeling complex, including *INO80*, *ARP8*, *ARP4*, *ACT1*, *RVB1*, and *RVB2*, some of which are more responsive to the extracts (Figure 1). Although none of these genes likely correspond to the target of virgineone, they seem to reflect the stress responses (at different levels, e.g., transcription, heat-shock, and drug tolerance responses) elicited by the antiproliferative effect of this compound such that heterozygosity at these loci results in reduced growth.

Production of 1 by Lachnum virgineum and Other Lachnum Strains. The presence of **1** in the other extract (F-230,308) was confirmed by HRLCMS (data not shown), as predicted by the almost identical CaFT profiles (Figure 1), demonstrating the dereplication potential of the assay to correctly predict the major bioactive components within complex natural product mixtures. Once the chemical properties of **1** were characterized, database matching was performed on new antibiotic extracts using an in-house application where the DAD, retention time, and POS and NEG mass spectra of the active samples were compared to the UV–LC–MS data of the authentic standard stored in a proprietary database. An additional seven strains from the United States, the Republic of Georgia, and Spain were recognized as producing the same tetramic acid (**1**) (Supporting Information, Table S1). DNA barcoding with the 28S rDNA indicated that these strains were all highly related and possibly conspecific, although they originated from widely different geographic locations. This group of strains also included an eighth apparently conspecific strain (F-262,581) that showed antibiotic activity against *S. aureus*, but in which **1** was not detected (Supporting Information, Table S1, Figure S2). None of these strains sporulated in agar culture. They were generally characterized as relatively slow growing, with waxy to appressed, pale buff to whitish gray mycelial colonies, and their identifications were not obvious. For the most part, they were associated with living plant or decaying plant material. Only F-265,955 was obtained from an unidentified lichen thallus (Supporting Information, Table S1). The relative placement in the 28S barcode tree indicated that these fungi are members of the Helotiales and belong to the genus *Lachnum* (Supporting Information, Figure S2). Similarity searches with ITS sequences from F-230,270, the original producing strain from Argentina, indicated that it may be conspecific with strains identified as *Lachnum virgineum*.

A large number of structurally diverse tetramic acid derivatives have been isolated from a variety of organisms. They have demonstrated antibacterial, antiviral, and antineoplastic activities; however, the precise mechanisms of action have not been determined for most of them.¹⁸ Antifungal activities have been described for only a few tetramic acids.^{19–21} Isolation of tetramic acid **1** was based on its intrinsic antifungal activity and the distinct mechanistic profile in the *C. albicans* fitness test. Virgineone (**1**) contains a tyrosine-derived tetramic acid, a C-22 oxygenated chain, and a β -mannose, and is active against a broad spectrum of fungal pathogens. Although the molecular mechanism of virgineone has not been established, the CaFT profiles suggest that its antiprolif-

erative activity elicits multiple stress responses in *C. albicans*. Furthermore, the cytotoxicity of virgineone is not restricted to fungi.

The discovery of **1** was achieved by chemogenetic profiling of crude natural products, in the form of extracted fermentation broths. In the CaFT, the biological activities in the unfractionated extracts are detected on the basis of induced growth variation in heterozygous deletion strains that cover a large fraction of the *C. albicans* genome. By comparing the profiles of natural products in question with those of known bioactive molecules, it is possible to discern the signature chemotypes present in the crude extract based on deduced bioactivities. This approach is particularly fruitful when combined with natural products from new sources. As demonstrated in this report, distinct CaFT profiles can reflect distinct biological activities, which, in turn, suggest distinct chemotypes and, likely, chemical entities in the extracts. We believe that the genome-wide fitness test affords a solution to biologically dereplicate crude extracts such that chemical resources can be allocated to those that are most likely to contain new chemical entities.

Experimental Section

General Experimental Procedures. Optical rotations were recorded with a Perkin-Elmer 241 polarimeter. UV spectra were recorded on a Perkin-Elmer Lambda 35 spectrometer. IR spectra were recorded with a Perkin-Elmer Spectrum One FT-IR spectrophotometer. All NMR spectra were recorded with a Varian Unity 500 (^1H , 500 MHz; ^{13}C , 125 MHz) spectrometer in $\text{DMSO}-d_6$ or CD_3OD . Chemical shifts are reported in δ (ppm) using residual solvent signals (for $\text{DMSO}-d_6$: δ_{H} 2.53 and δ_{C} 39.51 ppm; for CD_3OD : δ_{H} 3.30 and δ_{C} 49.00) as internal standards. ^1H , ^{13}C , COSY, DQF-COSY, DEPT, gHSQC, gHMBC, and TOCSY spectra were measured using standard Varian pulse sequences. LRMS data were recorded on an Agilent 1100 MSD with ES ionization, and HREIMS were obtained on a Thermo Finnigan LTQ-FTMS spectrometer. An Agilent HP 1100 instrument was used for analytical HPLC.

Fungal Material. The fungal strain F-230,270 (E-000509065, Merck Research Laboratory) was isolated from an unidentified plant collected in the province of Santa Cruz, Argentina (Supporting Information, Table S1). Additional *Lachnum* strains that produced virgineone are listed in Table S1 (Supporting Information). Strains were maintained as frozen mycelium in 10% glycerol at -80°C .

Fermentations in Nutritional Microarrays and Scale-up for Isolation. Our screening strategy relied on high-throughput generation of 1 mL-scale extracts of organisms grown under varied fermentation parameters followed by assay for antibiosis caused by cell-penetrable molecules using bioassays with *C. albicans* and *Staphylococcus aureus*. Organism-and-medium combinations yielding extracts with a minimum potency and activity spectrum were scaled up to provide larger fermentations suitable for profiling in the CaFT, further processing for an extract library, and for chemical fractionation, if needed. The strategy and protocols for fermentation of fungi on nutritional microarrays have been described previously.⁵ Each week, 160 to 240 fungal strains were selected for fermentations. These fungi were grown 2 to 3 weeks in 60 mm Petri dishes containing YM agar (Fluka or Difco malt extract 10 g, Difco yeast extract 2 g, agar 20 g, distilled H_2O 1000 mL). Three to four mycelial discs were cut from each 60 mm plate. Mycelia discs were crushed in the bottom of tubes (25×150 mm) containing 8 mL of SMYA medium (Difco neopeptone 10 g, maltose 40 g, Difco yeast extract 10 g, agar 4 g, distilled H_2O 1000 mL) and two cover glasses (22 mm^2). Tubes were agitated on an orbital shaker (200 rpm, 5 cm throw), and rotation of the cover glasses continually sheared hyphae and mycelial disc fragments to produce homogeneous hyphal suspensions. Tubes were agitated 4 to 6 days at 22°C .

Hyphal suspensions from these tubes were transferred to master inoculum plates. Master plates of fungal inoculum were used to inoculate 8-media nutritional arrays in a ten-column \times eight-row pattern.⁵ Nutritional arrays were grown statically 21 days at 22°C .

The detection of antifungal activity from strain F-230,270 originated from a 1 mL fermentation in the medium SCAS (soluble starch 40 g; casein hydrolysate 5 g; KH_2PO_4 0.5 g; $\text{MgSO}_4 \cdot 7\text{H}_2\text{O}$ 0.5 g; $\text{FeSO}_4 \cdot 7\text{H}_2\text{O}$ 0.01 g; distilled H_2O 10 000 mL). This fermentation was scaled up to 1 L by growing F-230,270 in 500 mL flasks with 150 mL of liquid SCAS agitated at 220 rpm, 22°C for 22 days. The liquid

fermentations were extracted with an equal volume of acetone and pooled. A 4 mL aliquot was frozen and tested in the CaFT, and the remaining extract was used for isolation of active metabolites.

Genome-Wide *Candida albicans* Fitness Test. The *C. albicans* fitness test was performed as described previously.⁸ Briefly, 5 mL cultures of the pool (at the initial OD_{600} of 0.025) were treated with antifungal actives (compounds and extracts) at multiple concentrations together with the mock treatment. The active inhibitory concentration of each culture was determined after 15 h at 30°C . Those with desirable ICs were retained and diluted to OD_{600} 0.05 with medium containing the antifungal active at the original concentrations. After another 23 h of growth, cell pellets were collected, and total genomic DNA was prepared. DNA samples of treated and mock cultures were PCR amplified using common primers that flank the strain-specific barcodes and labeled. Mixtures of labeled barcodes were hybridized against DNA microarrays. The relative responses (hypersensitivity and resistance) of each strain in the treated culture were appraised using an error-modeling statistic framework that involves a set of ~ 50 reference compounds and expressed by normalized z -scores of both up- and downstream barcodes (see ref 8 for details). For each strain, the z -score with higher absolute value was selected to compile the final list. Cluster 3.0 was used to analyze multiple fitness test experiments, the result of which was displayed with TreeView. Both are available at <http://bonsai.ims.u-tokyo.ac.jp/~mdehoon/software/cluster/software.htm>.

DNA Sequencing and Characterization of Fungal Strains. Total genomic DNA was extracted from mycelia grown on YM agar. The rDNA region containing the partial sequence of 28S rDNA including the D1 D2 variable domains was amplified with primers NL1 and NL4 or LROR and LR6. Sequences of 28S rDNA were used to generate a neighbor-joining tree (Supporting Information, Figure S1) that demonstrated the close relationships among the virgineone-producing strains and that they likely belong to the genus *Lachnum*. To achieve further phylogenetic resolution, the same genomic DNA samples were used to generate sequences of the intertranscribed spacer regions and 5.8S gene of the rDNA (ITS).

PCR reactions were performed following standard procedures (5 min at 93°C followed by 40 cycles of 30 s at 93°C , 30 s at 53°C , and 2 min at 72°C) with Taq DNA polymerase (Q-bioGene) following the procedures recommended by the manufacturer. The amplification products ($0.10 \mu\text{g}/\text{mL}$) were sequenced using the BigDye Terminators version 1.1 (Perkin-Elmer, Norwalk, CT) following the manufacturer's recommendations. For all the amplification products, each strand was sequenced with the same primers used for the initial amplification. Partial sequences were assembled using Genestudio software (Genestudio, Inc.), and consensus sequences were aligned by the same software. Neighbor-joining analyses were used to approximate phylogenetic relationships among strains.

Extraction and Isolation. An 1 L fermentation (pH 6.5) was extracted with 1 L of acetone and filtered through Celite, the filtrate was concentrated under reduced pressure to remove most of the acetone, and the extract was loaded onto a 50 cm^3 Amberchrom column packed in H_2O . The column was eluted with a 100 min linear gradient of $\text{H}_2\text{O}/\text{MeOH}$ at a flow rate of 5 mL/min followed by 20 min elution with MeOH. The fractions eluted with 80–100% MeOH showed antifungal activity. These fractions were combined, concentrated under reduced pressure to remove organic solvents, and lyophilized to yield 650 mg of material. This material was fractionated on a 500 cc Sephadex LH20 column packed and eluted with MeOH. The activity was spread and eluted in 0.5 to 1 cv (column volume), which upon concentration produced 650 mg of material, suggesting no separation. This material was purified by RP-HPLC using a Zorbax C_8 (250×21.2 mm) column at a flow rate of 12 mL/min with a 45 min linear gradient of 10–90% aqueous CH_3CN with 0.1% TFA. Fractions 22–25 were pooled from six independent HPLC runs and lyophilized to afford 326 mg (326 mg/L) of virgineone (**1**) as a colorless powder: $[\alpha]_{\text{D}}^{23} -95.7$ (c 0.3, MeOH); UV (MeOH) λ_{max} 201.4 (log ϵ 4.36), 229 (4.13), 242 sh (4.07), 281 (4.22) nm; IR (ZnSe) ν_{max} 3340, 2925, 2853, 1604, 1515, 1479, 1228, 1073, 1026 cm^{-1} ; ^1H and ^{13}C NMR data, see Table 1; ESIMS m/z 750 $[\text{M} + \text{H}]^+$; HRESIFTMS m/z 750.4423 (calcd for $\text{C}_{40}\text{H}_{63}\text{NO}_{12} + \text{H}$, 750.4384), 588.3881 (calcd for $\text{C}_{34}\text{H}_{53}\text{NO}_7 + \text{H}$, 588.3900).

Hydrolysis of Virgineone. A solution of **1** (6 mg) in 6 N methanolic HCl (1 mL) was heated at 60°C for 2 h. The reaction mixture was concentrated to dryness, redissolved in MeOH, and separated on a reversed-phase preparative HPLC using a Zorbax C_8 (250×21.2 mm) column at a flow rate of 12 mL/min with a 45 min linear gradient of

10–90% aqueous CH₃CN with 0.1% TFA. The fraction eluting at 20 min was lyophilized to afford 3 mg of **2** as a colorless powder: [α]_D²³ –60 (c 0.3, MeOH); UV (MeOH) λ_{\max} 201.4 (log ϵ 3.94), 229 (3.72), 242 sh (3.66), 281 (3.88) nm; IR (ZnSe) ν_{\max} 3248, 2928, 285X, 1616, 1511 cm⁻¹; HRESIFTMS m/z 588.3886 (calcd for C₃₄H₅₃NO₇ + H, 588.3900), 400.2121 (calcd for C₂₃H₃₀NO₅, 400.2124), 372.2172 (calcd for C₂₂H₃₀NO₄, 372.2175).

Antifungal Assay. The MIC (minimum inhibitory concentration) against each fungal strain was determined as previously described.²² Cells were inoculated at 10⁵ colony-forming units/mL followed by incubation at 37 °C for 20 h with a 2-fold serial dilution of compound in the growth medium.

In Vivo Efficacy Assay. Mice were infected iv (lateral tail veins) with *Candida albicans* MY1055 at 2.51 × 10⁴ cfu/mouse. Five DBA/2 mice in each group were treated with virgineone (**1**) formulated in 5% DMSO in sterile distilled water and treated at 100 and 50 mg/kg twice daily by ip administration. Mice were observed for mortality and general health for 4 days after challenge. At day 4 after challenge mice were euthanized, both kidneys were aseptically removed, placed in sterile Whirl-Pak bags, weighed, and then homogenized in 5 mL of sterile saline. Kidney homogenates were then serially 10-fold diluted in sterile saline and plated on SDA. Plates were incubated at 35 °C and counted after 30 to 48 h. Colony forming units (cfu) per gram of kidney were determined and counts from treatment groups compared to counts from sham-treated controls using a paired two tailed *t*-test (Excel).

Acknowledgment. We thank M. Arocho, K. Calati, K. Ferguson, and J. Occi for the preliminary isolation and assay support.

Supporting Information Available: ¹H and ¹³C NMR, description of other producing strains (Tables S1), and phylogenetic tree (Figures S1 and S2). This material is available free of charge via the Internet at <http://pubs.acs.org>.

References and Notes

- Hof, H. *Eur. J. Clin. Microbiol. Infect. Dis.* **2008**, *27*, 327–34.
- Zonios, D. I.; Bennett, J. E. *Semin. Respir. Crit. Care Med.* **2008**, *29*, 198–210.
- Gallis, H. A.; Drew, R. H.; Pickard, W. W. *Rev. Infect. Dis.* **1990**, *12*, 308–29.
- Georgopapadakou, N. H. *Expert Opin. Investig. Drugs* **2001**, *10*, 269–80.
- Bills, G. F.; Platas, G.; Fillola, A.; Jimenez, M. R.; Collado, J.; Vicente, F.; Martin, J.; Gonzalez, A.; Bur-Zimmermann, J.; Tormo, J. R.; Pelaez, F. *J. Appl. Microbiol.* **2008**, *104*, 1644–58.
- Haselbeck, R.; Wall, D.; Jiang, B.; Ketela, T.; Zyskind, J.; Bussey, H.; Foulkes, J. G.; Roemer, T. *Curr. Pharm. Des.* **2002**, *8*, 1155–72.
- Roemer, T.; Jiang, B.; Davison, J.; Ketela, T.; Veillette, K.; Breton, A.; Tandia, F.; Linteau, A.; Sillaots, S.; Marta, C.; Martel, N.; Veronneau, S.; Lemieux, S.; Kauffman, S.; Becker, J.; Storms, R.; Boone, C.; Bussey, H. *Mol. Microbiol.* **2003**, *50*, 167–81.
- Xu, D.; Jiang, B.; Ketela, T.; Lemieux, S.; Veillette, K.; Martel, N.; Davison, J.; Sillaots, S.; Trosok, S.; Bachewich, C.; Bussey, H.; Youngman, P.; Roemer, T. *PLoS Pathog.* **2007**, *3*, e92.
- Jiang, B.; Xu, D.; Allocco, J.; Parish, C.; Davison, J.; Veillette, K.; Sillaots, S.; Hu, W.; Rodriguez-Suarez, R.; Trosok, S.; Zhang, L.; Li, Y.; Rahkhoodae, F.; Ransom, T.; Martel, N.; Wang, H.; Gauvin, D.; Wiltsie, J.; Wisniewski, D.; Salowe, S.; Kahn, J. N.; Hsu, M. J.; Giacobbe, R.; Abruzzo, G.; Flattery, A.; Gill, C.; Youngman, P.; Wilson, K.; Bills, G.; Platas, G.; Pelaez, F.; Diez, M. T.; Kauffman, S.; Becker, J.; Harris, G.; Liberator, P.; Roemer, T. *Chem. Biol.* **2008**, *15*, 363–74.
- Parish, C. A.; Smith, S. K.; Calati, K.; Zink, D.; Wilson, K.; Roemer, T.; Jiang, B.; Xu, D.; Bills, G.; Platas, G.; Pelaez, F.; Diez, M. T.; Tsou, N.; McKeown, A. E.; Ball, R. G.; Powles, M. A.; Yeung, L.; Liberator, P.; Harris, G. *J. Am. Chem. Soc.* **2008**, *130*, 7060–6.
- Rodriguez-Suarez, R.; Xu, D.; Veillette, K.; Davison, J.; Sillaots, S.; Kauffman, S.; Hu, W.; Bowman, J.; Martel, N.; Trosok, S.; Wang, H.; Zhang, L.; Huang, L. Y.; Li, Y.; Rahkhoodae, F.; Ransom, T.; Gauvin, D.; Douglas, C.; Youngman, P.; Becker, J.; Jiang, B.; Roemer, T. *Chem. Biol.* **2007**, *14*, 1163–75.
- Singh, S. B.; Zink, D. L.; Goetz, M. A.; Dombrowski, A. W.; Polishook, J. D.; Hazuda, D. J. *Tetrahedron Lett.* **1998**, *39*, 2243–46.
- Wangun, H. V. K.; Dahse, H.-M.; Hertweck, C. *J. Nat. Prod.* **2007**, *70*, 1800–03.
- Wright, A. D.; Osterhage, C.; Konig, G. M. *Org. Biomol. Chem.* **2003**, *1*, 507–10.
- Schmidt, K.; Riese, U.; Li, Z.; Hamburger, M. *J. Nat. Prod.* **2003**, *66*, 378–83.
- Imai, J.; Yahara, I. *Mol. Cell. Biol.* **2000**, *20*, 9262–70.
- Nobile, C. J.; Mitchell, A. P. *Curr. Biol.* **2005**, *15*, 1150–55.
- Schobert, R.; Schlenk, A. *Bioorg. Med. Chem.* **2008**, *16*, 4203–21.
- Gunasekera, S. P.; Gunasekera, M.; McCarthy, P. *J. Org. Chem.* **1991**, *56*, 4830–33.
- Wang, C. Y.; Wang, B. G.; Wiryowidagdo, S.; Wray, V.; van Soest, R.; Steube, K. G.; Guan, H. S.; Proksch, P.; Ebel, R. *J. Nat. Prod.* **2003**, *66*, 51–6.
- Hellwig, V.; Grothe, T.; Mayer-Bartschmid, A.; Endermann, R.; Geschke, F. U.; Henkel, T.; Stadler, M. *J. Antibiot (Tokyo)* **2002**, *55*, 881–92.
- Bartizal, K.; Scott, T.; Abruzzo, G.; Gill, C.; Pacholok, C.; Lynch, L.; Kropp, H. *Antimicrob. Agents Chemother.* **1995**, *39*, 1070–76.

NP800511R